PÁZMÁNY PÉTER CATHOLIC UNIVERSITY

ROSKA TAMÁS DOCTORAL SCHOOL OF SCIENCES AND TECHNOLOGY

fides et ratio

RADELECZKI Balázs

Controlling cyclic motor tasks for movement rehabilitation after spinal cord injury

PhD Dissertation

Thesis Supervisor:

LACZKÓ József, PhD

2026

1 Introduction

The natural human locomotion can not be discussed without the understanding of the cyclic human limb movements. In running, crawling, swimming, climbing and even in case of walking or hopping, the arms have also an important roles alongside the legs.

Even those, who have "just" partially malfunctioning limb or limbs, have many difficulties to carry out everyday tasks, including locomotion. Therefore the rehabilitation or the substitution of the limbs are in the focuses of the clinical rehabilitation and bionics studies.

The human cyclic limb movements are also interesting from the biological point of view. The human gait, both walking and running are unique among the bipedal locomotions across all the living creatures.

In recent decades, it has frequently been questioned to what extent human upper and lower limb movements are differentially or independently controlled by the central nervous system, in contrast to other vertebrates, which in many cases exhibit coupled or dependent motor control between limbs during locomotion.

In this thesis, this question is addressed from the perspectives of both motor control and the clinical implications for the medical rehabilitation of patients with incomplete spinal cord injury.

1.1 From cycling to walking rehabilitation

Restoration of lost walking abilities after spinal cord injury is one of the main goals of Spinal Cord Injury (SCI) treatments and research. According to the literature, approximately 2/3 of the patients with SCI had incomplete

Spinal Cord Injury (iSCI) [1], [2]. In these cases, partial functionalities of the legs are observed, and the residual neural connections might be utilized for gait rehabilitation. The improvement of walking of iSCI persons would have a beneficial influence on the personal lives of the patients and social and economic systems.

Walking training for the patients requires sufficient force to stand up the body and keep it in motion. Furthermore, it demands realistic proprioception and balance. Many SCI persons lack these abilities. Thus, rehabilitation aims to strengthen and train the musculoskeletal system while protecting and enhancing the activity of the remaining neural pathways through neural plasticity. The earlier and the more efficiently we start to train the musculoskeletal system and stimulate the remaining neural pathways, the better recovery is expected. It is crucial to find the most effective rehabilitation protocols. The use of limb cycling training may be a good choice as it may improve walking functions [3].

In the gait rehabilitation of stroke survivors, the application of cyclic and pedaling movements was addressed to mimic similar movements to walking as soon as possible during the rehabilitation therapy [4].

There are other publications which also highlighted the analogy of walking and leg cycling [5] or "arm & leg" cycling [6]. These exercises do not require much muscle strength as the body weight does not have to be supported by the patients' muscles. So, the application of arm and leg cycling in the gait rehabilitation of iSCI patients seems to be a beneficial choice and it is essential for the spinal cord injured population to do such exercises to train walking functions.

Cycling exercises can be assisted or driven by electrical stimulation techniques as well. A common application of electrical stimulation with leg cycling is Functional Elctrical Stimulation assisted leg cycling (Functional Electrical Stimulation assisted leg cycling (FES cycling)).

Our recent study shows [J1] that even in the early subacute phase of iSCI, FES cycling can have a beneficial effect on improving the power output of the participants during cycling training. Since walking also demands significant muscle strength and motor control, this technique appears to be a useful in gait rehabilitation as a supplementary training.

Yaşar et al. studied the effects of FES cycling in the case of chronic iSCI participants ($n = 10$). Each participant had 1 hour-long training session, 3 days per week for 12 weeks. They found that the Functional Independence Measure (FIM) significantly increased [7]. Gait parameters such as gait velocity, cadence, and step length increased but not significantly [8].

Duffell further developed this method with the modulation of the stimulation pattern according to the crank torque, during pedaling. This system was extended with biofeedback based virtual reality [9]. Their study involved 11 sub-acute iSCI participants. The training consisted of $3 \times (20 - 45)$ minutes of FES cycling training sessions per week. The training lasted 4 weeks for each participant. The participants also had sporadic improvement according to the Modified Ashworth Scale (MAS) and a slight improvement in the mobility score of Spinal Cord Independence Measure (SCIM).

If Functional Electrical Stimulation (FES) cycling is supplemented by simultaneous voluntary arm cycling, it may be a more efficient form of training than conventional FES cycling performed only with the legs. This combined exercise of the arms and legs is called hybrid Functional Electrical Stimulation cycling (hybrid FES cycling).

The paper of Zhou et al. showed that hybrid FES cycling improves more the walking abilities of iSCI participants compared to simple FES cycling [3]. In their study, they involved seven ($n = 7$) iSCI participants in the hybrid FES cycling and eight ($n = 8$) iSCI participants in the FES cycling. All participants received intensive training: 5×1 hour training sessions per week for 12 weeks. Their results proved that a significantly better improvement in walking ability can be achieved with hybrid FES cycling compared to FES cycling. The underlying reason behind the beneficial impact of upper limb cycling on gait rehabilitation remains unclear, but the authors hypothesize that rhythmic movement of the upper and lower limbs shares common neural pathways, and their activation may induce favorable changes in walking patterns.

The intensity of the cycling training differs when the above-mentioned studies are considered. When planning training protocols for cycling, the intensity is an important question. Should we need high-intensity training (frequent and long training sessions) to get walking improvements as a result of arm and leg cycling training?

1.2 Common motor control of the arms and legs during cycling

Zehr et al. [10] investigated the effect of leg cycling on the arm H-reflex and on the activation of corticospinal neural projections to the arm. Leg cycling suppressed the H-reflex of the lower arm muscle, the flexor carpi radialis, even when the arm was relaxed or isometrically contracted during foot pedaling.

Sakamoto et al. found that during simultaneous arm and leg cycling, the changes of the arm cycling speed had no effect on the pedaling speed of the legs, but if the pedaling of the legs was slowed or accelerated, the pedaling speed of the arms also changed [11]. Sakamoto et al. investigated how arm and leg cycling in a sitting or standing position modulates the cutaneous reflexes of the arms and legs in a phase-dependent manner. They found that the magnitude of the reflexes in both arms and legs was modulated by the position of the pedals. In addition, there was no difference in the reflex changes occurring between the lower and upper limbs and the amplitude of the ipsilateral limb reflexes between in-phase and anti-phase arm and leg cycling [12].

Zhou et al. [13] demonstrated that the motor activation potential (MAP) evoked by transcranial magnetic stimulation of the corticospinal tract, in the vastus lateralis leg muscle is significantly greater when the participant does arm cycling with resting legs than when all four limbs are relaxed in a static position. No significant difference was found in case of participants with iSCI who had very limited walking ability (less than 0.31 m/s). From this results, they concluded that arm cycling movements modulate corticospinal motor control of the lower extremities and this control is impaired in incomplete spinal cord injured participants.

In the second part of the same publication, the authors investigated the effects of 12 weeks of FES-assisted simultaneous arm and leg cycling training (1 hour/day, 5 days/week). They found that patients had significantly higher motor activation potentials (MAPs) through the corticospinal tract in the vastus lateralis leg muscle after training than before. So, hybrid FES cycling has a beneficial effect on the functional recovery of corticospinal neural pathway.

These studies highlight strong connections between upper and lower limb cycling at the level of reflex pathways, as well as the descending (corticospinal, cervicospinal) and ascending (cervicospinal) pathways of the spinal cord. However, to the best of our knowledge, no study has yet investigated this question at the organizational level of muscle synergies. Namely, it remains unclear whether the upper and lower limbs influence each other at the level of neuromuscular coordination.

2 Objectives

Question 1, Is there a detectable neural interlimb coordination between the arms and legs during simultaneous arm cranking and leg cycling motor tasks?

To investigate this question, I applied two different approaches. In the first, I examined whether the neural interlimb coordination between the arms and legs could be replaced by artificial control. In the second approach, I examined how the synergistic coordination of the arm muscles during arm cycling depends on whether the task is performed without leg cycling or simultaneously with leg cycling.

Objective 1a,

- Collect and process Electromyographic (EMG) and kinematic data from healthy individuals performing arms and legs cycling simultaneously.
- Implement a regression-based estimation method using neural network training to predict the EMG activity of selected knee flexor and extensor muscles from EMG signals recorded from the arm muscles.
- Apply threshold-based methods to compute unipolar control signals suitable for FES cycling.

Objective 1b,

- Collect and process Electromyographic (EMG) and kinematic data from healthy individuals performing cycling tasks under two conditions: (1) using the arms only, and (2) using both the arms and legs simultaneously.

- Extract muscle synergies by applying non-negative matrix factorization (NNMF) to the electromyographic (EMG) data.
- Structure the extracted synergy weights and activation coefficients (control signals) and perform quantitative comparisons to evaluate differences or similarities across conditions.

Question 2, How do the ground reaction forces during walking change in case of incomplete spinal cord injured participants who, in addition to the conventional rehabilitation therapies, participated in simultaneous voluntary arm cranking and functional electrical stimulation-assisted leg cycling (hybrid FES cycling) training?

Objective 2,

- Perform gait assessments on participants with incomplete spinal cord injury at three time points: prior to, midway through, and following the hybrid FES cycling training program.
- Collect Ground Reaction Force (GRF) data and their derived measures, center of pressure (CoP) trajectories, from individuals with incomplete spinal cord injury.
- Acquire gait specific reference kinematic and EMG measurements from individuals with incomplete spinal cord injury.
- Extract and compute relevant biomechanical parameters from the force plate measurements and corresponding reference data.
- Quantitatively compare the extracted biomechanical and reference parameters before and after the hybrid FES cycling training.

3 Methods

3.1 Arm & leg cycling - neural network

3.1.1 Participants

In this exploratory study, four adults (24-30 years old, 2 women, 2 men) were enrolled. Before the measurements, participants gave their written informed consent to take part in this study, which was approved by The Ethical Committee of the National Institute of Medical Rehabilitation, Budapest.

3.1.2 Recorded Muscles

The list of the recorded muscles is the following:

right gluteus maximus (GM), right rectus femoris (RF), right vastus medialis (VM), right vastus lateralis (VL), right biceps femoris (BF), right tibialis anterior (TA), right gastrocnemius medialis (GM), right gastrocnemius lateralis (GL), right anterior deltoid (AD), right posterior deltoid (PD), right biceps brachii (BB), right triceps brachii (TB), right flexor carpi radialis (FCR), and right (BR)

3.1.3 Exercise and Measurement protocol

The participant was seated comfortably on a backrest chair at the front of the Motomed Viva2 hybrid arm and leg cycle ergometer. At the beginning of the measurements, we independently measured the arms and the legs cycling while the participants had to keep a pedaling speed of 60 rpm (revolutions per minute). To give the participants feedback about the cycling speed, audio signals were provided with the required frequency. After that, the user had to cycle synchronously with his upper and lower limbs at the same speed of 60 rpm. When it was finished, the protocol continued with similar exercises, where the only difference was that the task had to be performed asynchronously.

3.1.4 Eletromyogram signal processing

The EMG signals were filtered by a fourth-order Butterworth filter (bandpass 20–500 Hz) and a notch filter (50 Hz) and then smoothed by root mean square (RMS) with a window length of 80 samples (66.6 ms). In the last preprocessing step, we concatenated 30-s EMG records from each participant for synchronous and asynchronous cycling separately. Thus, we had two time series, each with a length of 4×30 s. Then, these time series were amplitude normalized to the range [0–1]. For normalization, we applied the rescale() MATLAB function. This was beneficial because the activation functions of the neural network have a similar range. This method restricts the neural network weights, which helps the learning method.

Eight muscles were used for the neural network training. We used all six EMG channels of the right arm as an input for the neural network, and two muscles, the right rectus femoris (R. Rect. Fem.) and right biceps femoris (R. Bic. Fem.), were used as targets for the output prediction. The reduction of the lower limb channels is based on the following consideration. The aim was to use only the EMG signals of the arm muscles for the prediction of lower limb muscle activities. Hence, we cannot apply the lower limb EMG as a direct input of the transformation.

The illustration of the mapping is found in Figure 3.1.

We also reduced the record size by under sampling the filtered and smoothed time series. During the under sampling, we selected every 30^{th} sample for the network training, which was necessary to perform reasonable computation times in our resources. In addition to the computational speed increase, it could also be beneficial for the learning capability of the system. This method highlights the evolution of the main features over time.

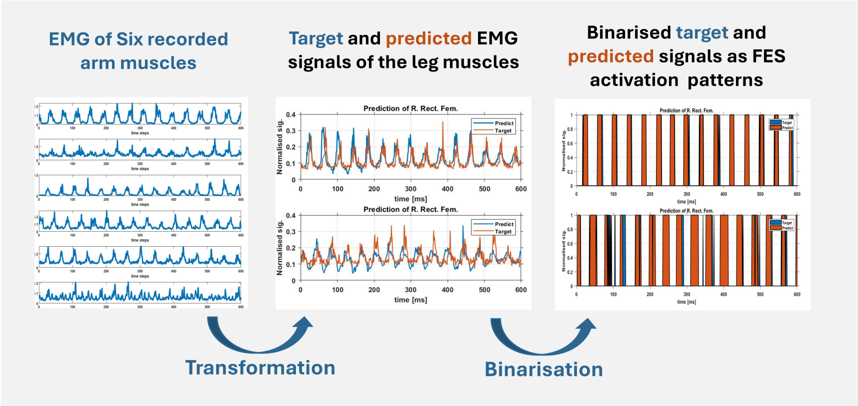

Figure 3.1: Calculation steps for FES onset-offset timings. The neural network predicts knee flexor and extensor EMG activity from EMG signals of six arm muscles, which are then binarized into FES activation patterns.

3.1.5 Neural network model

For the arm & leg cycling – neural network training tasks, we used nonlinear auto-regressive exogenous (NARX) neural networks. This neural network is a subtype of the recurrent neural networks. This means that the output of the network is fed back to the system as an input. Another important expression is "exogen," which refers to the type of inputs. The terminology is used because this network — in every step — has one or more external inputs beside the feedback. Our model uses the actual and the last 14 recorded values of the six arm muscle activities (EMG channels) for external input. For internal input, it uses the feedback of the actual and the last 24 recorded output values for the two output channels.

These output values represent the predictions of the R. Rect. Fem. and R. Bic. Fem. EMG signals. The description of the system is mathematically formalized in Equation 3.1.5, where $u(t)$ and $y(t)$ represent the input and output of the network at time t. D_u and D_y are the input and output orders, respectively, and the function f is a nonlinear function [14].

$$y(t) = f[u(t - D_u), \ldots, u(t-1), u(t), y(t - D_y), \ldots, y(t-1)] \tag{3.1}$$

For the task, we used three hidden layers with the following number of neurons from the first to the third layer: 10, 7, and 5. In the hidden layers, we applied sigmoid activation functions. A hidden layer is fully connected with the previous and the next layers. The output layer contains two neurons with an identity transfer function where the predicted outputs are fed back to the first hidden layer. The neural network is illustrated in Figure 3.2.

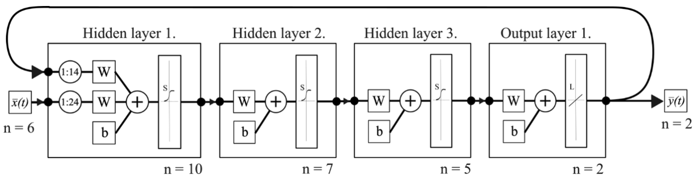

Figure 3.2: The applied neural network for the task. The neural network has three hidden layer with n = 10, 7, 5 number of neuron and one output layer with two neurons. The layers were fully connected. The W letters denote the weight matrices and the b letters are the bias values. The direction of the information flow is denoted by the arrows.

3.1.6 Training of the network model

For neural network learning, we used the Electromyogram (EMG) records of cycling exercises. For each condition, equal size recordings of four participants were concatenated, and using these time series, we trained the neural network for each condition separately. The network training used the Levenberg-Marquard built-in method for optimization for 80 epochs.

The training error was measured by a mean square error (MSE) calculation. For the program testing, 8×10 cross-validation was applied. This means that the data sequences that contain the records of four participants are divided into eight subgroups. From these eight subgroups, we constructed eight different training and testing groups in the following way: the test set contains only one subgroup, while the training set includes all the remaining seven subgroups.

With this kind of arrangement, eight different training and test sets can be constructed. After the construction of these learning sets, the learning algorithm was applied 10 times. In each round, the program calculated its prediction accuracy for the thresholded signals. Because learning is not a deterministic process, it produces different outcomes for 10 different attempts, which is why we can obtain 8×10 quantitative results at the end. Finally, these results were aggregated by the arithmetic mean for each quantity and learning set. "We evaluated the generalization performance of the learning process with this method.

3.1.7 Thresholding for binary control signal construction

I show a simple construction of binary control signals derived from the predicted EMG of the target muscles. We calculated the normalized histogram of the selected EMG signal. For the normalization, we applied the total number of points in the EMG time series. The histogram is constructed with 200 bins. Then, we determined the threshold as a value that divides the samples of the signal into a predefined ratio among the area of the upper bounded values and the total area. This ratio was approximately 2/3.

To measure the accuracy of the binary activation patterns (predicted and target patterns), we calculated the average total phase difference in one 360°circle. It is formalized mathematically in the following way:

$$\text{Angle accuracy} = 360 - \frac{1}{N_{\text{cycle}}} \sum_{i=1}^{n} |\vec{y}_i - \vec{p}_i| \, \alpha_{\text{res}}, \tag{3.2}$$

$$\text{where } \vec{y}, \vec{p} \in \{0,1\}^n \text{ and } \alpha_{\text{res}} \in \mathbb{R}$$

where $\vec{y}$ is the thresholded target signal, $\vec{p}$ is the thresholded prediction, n is the length of the two time series, i is the actual coordinate, N_{cycle} is the number of cycles and α_{res} is the angular resolution of the method. This value can be obtained as 360°/(number of EMG points used in one circle).

3.2 Arm & leg cycling – muscle synergy analysis

3.2.1 Participants

Ten healthy women (age 22.2 ± 3.7 years, height 1.64 ± 0.06 m, weight 59.6 ± 5.3 kg) without any known orthopedic or neurological problems participated in this study and provided informed consent. All of them were right-handed and right-footed. The experiments were conducted in accordance with the Declaration of Helsinki. The Ethics Committee of the National Medical Institute for Rehabilitation, Hungary (presently Semmelweis University, Rehabilitation Clinic) provided approval for this research.

3.2.2 Recorded Muscles

The list of the recorded muscles is the following:

left and right anterior deltoid (AD), left and right posterior deltoid (PD), left and right biceps brachii (BB), left and right triceps brachii (TB), left and right extensor carpi radialis (ECR), left and right flexor carpi radialis (FCR)

3.2.3 Exercise and Measurement protocol

Each participant performed several cycling tasks on a MotoMed Viva2 (Reck GMBH, Betzenweiler, Germany) arm and leg cycle ergometer (Figure. 3.3). Each participant cycled with her arms against 2 different levels of arm crank resistance: low and moderate. Cycling was performed in 2 different modes: cycling only with the arms ("only-arm" mode) and cycling with both arms and legs ("arm & leg" mode). Therefore, each participant performed 4 different combinations of cycling: 2 cycling modes with 2 levels of resistance.

In the arm & leg cycling mode, each participant was asked to cycle with both arms and legs simultaneously, with the right arm cycling at the same cycling frequency and same phase of the left leg and to try to keep it synchronized.

For each combination of cycling, surface EMG signals were recorded for each side independently.

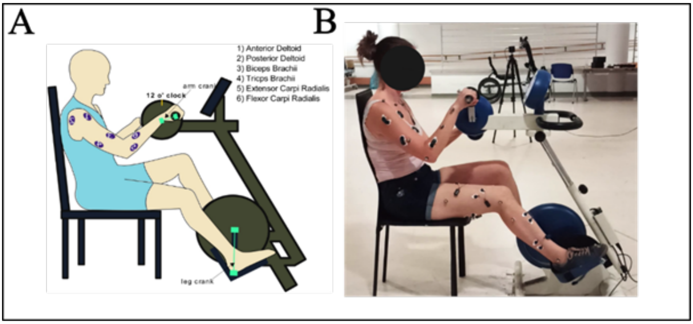

Figure 3.3: The schematic figure of the arm & leg cycling exercises. During the exercises six arm muscles were measured by electromyography. These muscles are highlighted in Panel A. The muscle activity of the left and right sides were recorded independently. Panel B: A real example of a participant sitting in front of the ergometer while performing an arm and leg cycling task.

The cycling frequency was predefined as 60 revolutions per minute (rpm). A 60-rpm audio feedback was provided by a metronome. For each setup, the participants cycled in total for three minutes. Short breaks (60 s) were taken between these 3-minute cycling trials to avoid muscle fatigue.

3.2.4 Kinematic signal processing

The vertical coordinates of the marker on the right handle of the ergometer were used for cycle segmentation. One cycle was defined as an interval between two consecutive 12 o'clock positions of the right crank. To determine these events, the findpeaks() MATLAB The MathWorks, Natick, MA, USA). function was applied to the time series. These positions were then used to segment the movement of both the right and left arms.

3.2.5 Electromyogram signal processing

All recorded EMG signals from each setup were band-pass filtered (25-300 Hz, 3^{rd} order Butterworth). We then applied a 2^{nd} order IIR Notch filter at 50 Hz on these filtered data. The mean signal value was subtracted from the EMG signals. Finally, the EMG signals were rectified and low-pass filtered at 5 Hz (3^{rd}-order Butterworth) to obtain the EMG envelopes [15], [16]. EMG envelopes were then time-normalized by resampling the data at each percentage of the cycle (101 points: 0-100).

EMG envelopes were analyzed on a cycle-by-cycle basis to identify outliers that needed to be removed.

On average, more than 60 cycles were retained for further analysis (across participants) for each setup. This number of cycles is considered adequate, based on the recommendation of Turpin et al. [17].

For each participant (10), the maximum of EMG envelopes of all cycles for each setup (8) and muscle (6) were found. Then for each muscle, the largest one of these 8 EMG maximum values was used to normalize all EMG time series for that muscle.

3.2.6 Synergy calculations

For each setup, concatenated EMG envelopes were combined into $m \times t$ (EMG_o) matrices, where m is the number of muscles (six, in this case) and t is the time base (number of concatenated cycles $\times 100$). Muscle synergies components were calculated applying a non-negative matrix factorization (NNMF) method [18] with MATLAB (The MathWorks, Natick, MA, USA). Mathematically, the algorithm is described as

$$EMG_o = WH + e = EMG_r + e \tag{3.3}$$

Where W is the $m \times n$ matrix specifying the weight of each muscle in each synergy, n is the number of muscle synergies, and H is the $n \times t$ matrix specifying the time-varying activation coefficients representing the recruitment of each synergy throughout the cycle. EMG_r is the matrix $m \times t$ resulting from the multiplication of W and H (reconstructed EMG envelopes), and e is the residual error. We considered 3 and 4 synergies ($n = 3, 4$) as input to the NNMF algorithm. For each n, NNMF was run 40 times, and the repetition with the smallest reconstruction error was selected. The minimum number of synergies required to guarantee an adequate reconstruction of the EMG signals was determined as the minimum number necessary to obtain a variability accounted for (VAF) greater than or equal to 90%, as done in other studies [5], [16], [19].

3.2.7 Synergy vector ordering

We applied max-normalization on the W synergy weight matrix [20]. We normalized each column of the W synergy matrix by the maximal value of the column. Synergy vectors (columns of W matrices) were then ordered for each participant and setup, based on their similarity to each other. We used the cosine similarity of the synergy weights as a metric of similarity [5], [16]. For each setup, we ordered the synergy vectors of each participant compared to a reference participant. Next, for each setup, corresponding synergy vectors were averaged across participants. Finally, we also ordered the averaged synergy vectors with respect to the reference condition (only arm cycling mode, low resistance, left side). The activation coefficients (H matrices) followed the order corresponding to the synergy vectors.

3.2.8 Statistical analysis

Our main goal was to explore the effects of different cycling combinations (mode or resistance) on muscle synergies. First, the normality of the synergy vectors was checked with Shapiro-Wilk test. Given that the data did not show a normal distribution, non-parametric statistical methods were used. The elements of the synergy vectors, i.e., the activation coefficients and the synergy weights, were analyzed with several different methods to strengthen our findings.

The activation coefficients were averaged across cycles for each participant and time normalized to 101 samples (0-100). The averaged activation coefficient array for each cycling setup was created as follows: number of participants x number of synergies x length of averaged cycle (10x4x101).

To examine the similarity between the different cycling combinations, Spearman rank test was applied on the averaged cycle of activation coefficients in participants, separately the four coefficients. To calculate the significancy (p-values) of the correlation and the effect size (Cohen's d), we applied Fisher-z transformation.

Moreover, we investigated also the differences between the cycling combinations on the mean activation coefficients. Statistical Parametric Mapping (SPM) vector-field analysis is an established method for quantitative correlation of biological time series (28).

For pairwise comparisons of the activation coefficients, non-parametric paired T-test was applied within the SPM with Bonferroni correction. We used the open sorce SPM library for MATLAB.

The synergy weights were also compared between the different cycling combinations. To analyze the similarity of the different cycling combinations in terms of synergy weights, cosine similarity was calculated between the averaged (across participants) synergy weights (29)

We also investigated the differences between the synergy weights in cycling combinations, applying Friedman test for the synergy weights of each muscle in the JASP statistical software (30). Conover post-hoc test was used (31), which is recommended after the Friedman test for pairwise comparisons (32). The significance level was set at a p value of 0.05, with the application of the Holm-Bonferroni correction.

3.3 Hybrid FES cycling training - walking assessment

3.3.1 Participants

Five male participants with subacute iSCI, who provided written consent prior to participate, are included in this study in accordance with the Declaration of Helsinki. The National Public Health Center, Budapest, Hungary, gave authorization, the Scientific and Research Ethics Committee of the Health Scientific Council approved the authorization for this research.

3.3.2 The Organization of the training

The participants had 2×30 minutes long hybrid FES cycling training sessions per week for 12 weeks. In each training session, they had to perform simultaneous FES-assisted lower limb cycling and voluntary arm cycling. Besides the training, the participants got conventional rehabilitation therapy. During the training, three walking ability assessments and three clinical assessments were taken: before the training program started, six weeks later, and when the training was completed. See Figure 3.4.

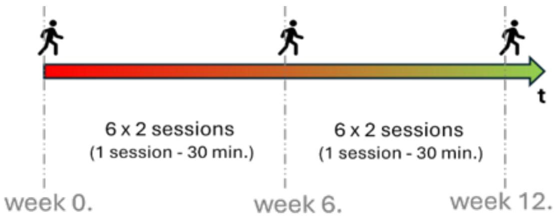

Figure 3.4: It illustrates the number of cycling training sessions and the distributions of the gait assessments of the participants. The human pictograms represent the biomechanical gait and clinical assessments.

3.3.3 The training sessions

All of the training sessions had the following specification: The physiotherapist assisted the participants in positioning themselves to the ergometer. Then, bipolar surface electrodes were placed on the quadriceps and hamstrings muscle groups on both legs. The exercises are illustrated at Figure 3.5. The stimulation frequency (30 Hz), and the pulse width (300 µs) were constant in each training session. The current amplitude was set and changed by the physiotherapist.

Figure 3.5: Clinical application of hybrid FES cycling training.

At the beginning of the session, five minutes of passive leg cycling was applied without electrical stimulation, when the ergometer's motor rotated the lower cranks. This was a warm-up period. Then, the participant performed 20 minutes of hybrid FES cycling.

The session was finished with 5 minutes of passive leg cycling to relax the leg muscles.

3.3.4 Recorded Muscles

The list of the recorded muscles is the following:

left and right rectus femoris (RF), left and right vastus lateralis (VL), left and right vastus medialis (VM), left and right semitendinosus (Smt), left and right biceps femoris (BF).

3.3.5 Gait assessment

Walking was performed at the preferred speed along a straight path over 3D force plates. In each assessment, we observed four walking trials.

The following parameters were analyzed: step length, step time, walking speed, and maxima of absolute values of 3 orthogonal components of ground reaction forces (mediolateral -x, posteroanterior -y, and vertical -z components of GRF), for each component separately. Euclidean lengths and total jerk of the Center of Pressure (CoP) progression curves were computed. After each assessment GRFs and CoPs were averaged across the stance phases of several steps for each side (from 4 walking trials, above the 3 force plates).

Beside the biomechanical parameter assessments, I wanted to quantify the repeatability and regularity of the EMG activity of the leg muscles during the walking since it gives us additional information of the neuro-muscular control of the patients.

The extended definitions of Shannon entropy on the EMG time series are good choices because it is a scalar quantity and despite that, it describes the general regularity of the time series. I calculated the Sample Entropy (SampEn) which was defined by Richman et al. [21], The preliminary results of the application of SampEn in our work have already been published [C1].

3.3.6 Electromyogram signal processing

During the SampEn analysis of the knee extensor and flexor muscles. First, the raw EMG signals were band-pass filtered between 25 - 350 Hz using a third-order Butterworth filter. Subsequently, the 50 Hz power line interference was attenuated using a third-order Butterworth notch filter with [49–51] Hz range. Finally, the signals were full-wave rectified and smoothed using the Root Mean Square (RMS) smoothing technique. A moving window of 61 samples (51 ms) was used, in accordance with recommendations found in the relevant literature [22]. The filtered and smoothed EMG signals were segmented into gait cycles, each defined as the interval between two consecutive left heel strikes. The EMG data corresponding to each gait cycle were linearly interpolated to a uniform length of 500 samples.

SampEn values were computed from each uniform length gait cycles for each muscle separately. The mean and standard deviation of the gained SampEn values were aggregated across the gait cycles. For the entropy calculation, the open-source sampen() MATLAB function developed by Richman et al. [23] was used. The parameters for the function were set to $m = 4$ and $r = 0.2$. The parameters were set according to our previous work [C1] which follows the best practices of the literature.

3.3.7 Kinematic signal processing

One step was defined as the event during two consecutive heel strikes of the legs. For the heel strike event detection, we used the left and right heel markers. The local minima of the time courses of the vertical (z-axis) coordinates of these markers correspond to the heel strikes. The step time is defined as the time difference between the two local maxima. The step length is calculated as the Euclidean distance of two heel strikes with respect to the forward-backward (y-axis) direction. The walking speed is calculated as the mean ratio of the step length and step time.

3.3.8 Dynamic signal processing

Ground Reaction Force components

The time courses of the absolute values of (x,y,z) components of 3D GRFs were investigated for each step. The maximum of each of these time series was selected in each step. Then the mean (μ_{cord}) and the standard deviation (SD_{cord}) of these values across steps and trials were calculated using Eq. 3.4 and 3.5.

$$\mu_{\mathrm{cord}} = \mathrm{mean}\left(\max_{1 \le t \le N}(|\mathrm{GRF}_{\mathrm{cord},t}|)\right) \tag{3.4}$$

$$SD_{\mathrm{cord}} = \mathrm{std}\left(\max_{1 \le t \le N}(|\mathrm{GRF}_{\mathrm{cord},t}|)\right) \tag{3.5}$$

Where $GRF_{cord} \in \mathbb{R}$ and $N, t \in \mathbb{N}$; N is the length of the time series in the actual step and t is the actual timestamp.

Center of Pressure progression

CoP curve length for each step is defined by the interval between the two greatest local maxima of the vertical GRF (z-axis). See Figure 3.6. These time points are associated with the events of loading and push-off. In these time intervals, we calculated the summed Euclidean distances between the recorded CoP points.

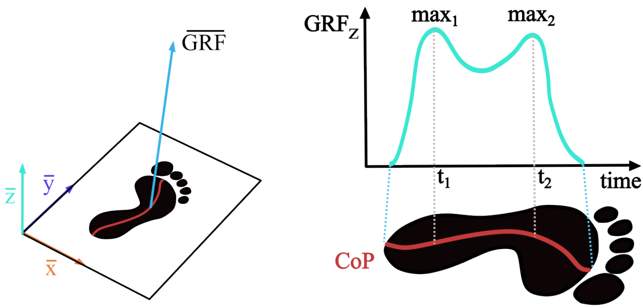

Figure 3.6: The connection between the Ground Reaction Forces (GRF) and the Center of Pressure (CoP). The CoP progression curve is created by the set of origin points of the GRF vector on force plate during stance phase of the walking.

Jerk computation

Time courses of CoP coordinates $[CoP_x(t), CoP_y(t)]$ and their derivatives with respect to time were computed, up to the third order. After each differentiation data were filtered by second order Butterworth filter with 10 Hz cut-off frequency. The total jerk of the CoP path trajectory was computed as follows:

$$J_{\text{total}} = \int_{t_1}^{t_2} (CoP_x'''(t))^2 + (CoP_y'''(t))^2 dt \tag{3.6}$$

Where $[t_1, t_2]$ is the studied time interval of the CoP progression, illustrated in Figure 3.6. $CoP_x(t)$, $CoP_y(t)$ represent mediolateral and posteroanterior components of the CoP displacement as function of time, $<,>$ denotes scalar product.

3.3.9 Statistical comparison of biomechanical parameters between the three assessments

To ensure statistical comparability, the distribution of the data was first assessed to determine whether it followed a normal or non-normal distribution. This was evaluated using the Shapiro–Wilk hypothesis test, with a standard significance level set at $p = 0.05$. The test was implemented using the open-source swtest() function available on the MathWorks website of MATLAB.

During the execution of the Shapiro–Wilk test, I found that nearly all examined parameters had non-normal distributions, regardless of whether the parameters were analyzed collectively or separately for the left and right legs, for different gait assessments. In cases where the data did not follow a normal distribution, a log-normalization was applied, followed by a repeated Shapiro–Wilk test. However, log-normalization did not result normal distributions in these cases. Consequently, to ensure consistency in the statistical analysis across parameters, sides (left and right), and gait assessments, all subsequent analyses were conducted using non-parametric statistical methods.

To compare the results obtained at week 0., 6., and 12., a non-parametric Friedman test was applied, using MATLAB's built-in friedman() function. The results of the Friedman test were followed by Bonferroni post hoc test. For this purpose, MATLAB's multicompare() function was utilized.

4 Results

4.1 Outcomes of arm & leg cycling - neural network

These results have been published in [J2], include prediction outcomes for synchronous and asynchronous hybrid cycling tasks. See Figure 4.1.

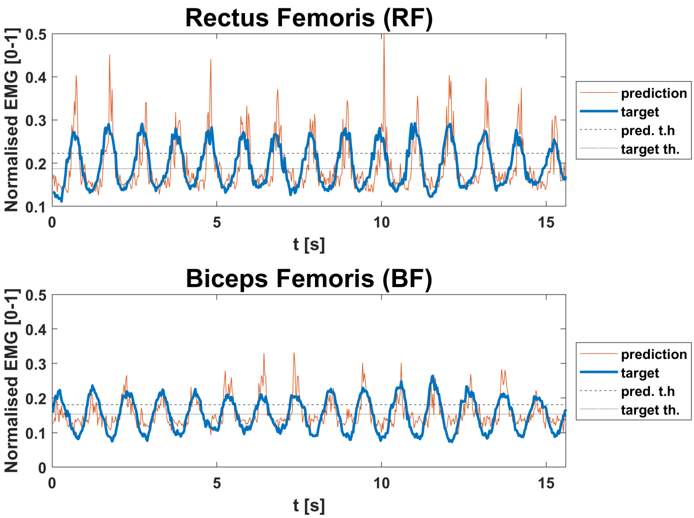

Figure 4.1: Normalized original (orange) and NARX-predicted (blue) EMG signals of the R. Rectus Femoris (top) and R. Biceps Femoris (bottom) during 15 asynchronous cycling periods. The model was trained on four participants using six right-arm EMG inputs; dotted lines indicate thresholds.

Subsequently, we illustrate the outcomes of the binarization process. We provide two representative examples of averaged binary matching values under the two distinct learning conditions, see Figure 4.2. The performance of the employed learning algorithm is quantitatively assessed by comparing the predicted binary signals to the corresponding target signals. These accuracy metrics are summarized in Table 4.1.

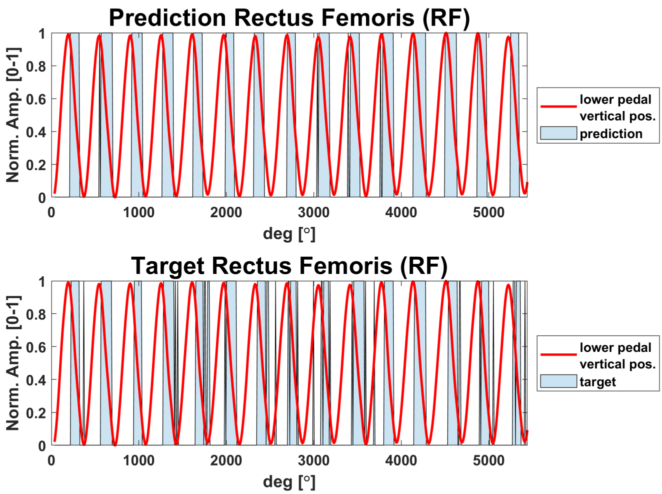

Figure 4.2: Measured (bottom) and predicted (top) binarized R. Rectus Femoris (RF) activity across 15 asynchronous cycles. The binary signal (blue) indicates activity above threshold. The red curve denotes pedal position.

Table 4.1: The table summarizes the mean performance and standard deviation of the binarized activation patterns...

Task	Muscle	P1	P2	P3	P4
Synchronous	r. rectus fem.	228° ± 26°	225° ± 31°	212° ± 19°	174° ± 43°
	r. biceps fem.	201° ± 15°	181° ± 24°	195° ± 20°	186° ± 30°
Asynchronous	r. rectus fem.	272° ± 36°	208° ± 31°	190° ± 27°	208° ± 41°
	r. biceps fem.	200° ± 29°	205° ± 14°	227° ± 17°	237° ± 35°

4.2 Outcomes of arm & leg cycling - muscle synergy analysis

4.2.1 Comparison of muscle synergies components

The results of the synergy calculations are shown in Figure 4.3. The average and standard error of the synergy weights (W) and coefficients (H) across the participants are illustrated.

We compared the cycling setups between low and moderate resistance and between the "only arm" and "arm & leg" cycling modes in level of activation coefficients and in synergy weights.

With respect to the activation coefficients, the results of similarity analysis the ϱ values based on Spearman rank test was presented with p-values and Cohen's d effect size in the Table 4.3. There was statistically significant high correlation between the cycling modes and resistance levels ($p < 0.05$, $d > 0.8$). Only in one case, in arm & leg cycling mode, the left arm was not significantly high in the correlation ($\varrho = 0.46$, $p = 0.09$, $d = 0.6$) between the two resistances.

The comparison of the activation coefficients using the SPM method did not reveal statistically significant differences between the setups. There was no significant difference between the resistances nor between the cycling modes.

Regarding synergy weights, the cosine similarity was presented between the cycling combinations, in the Table 4.2. The synergy weights between the low and moderate level of resistance were similar for left side, in two cycling modes, and for the right side for arm & leg cycling mode (cosine similarity was higher than 0.83). Only for third Synergy weights, in the right side, only arm cycling mode was the cosine similarity below 0.8 (0.76), which was the similarity threshold in other studies [24], [25].

Table 4.2: Cosine similarity of synergy weights. The setups were as follows: resistance – low (low) or moderate (mod), cycling mode – only-arm or arm&leg, and side – left or right side.

	Resistance				**Cycling mode**			
	left, only arm	left, arm &leg	right, only arm	right, arm &leg	left, low	left, mod	right, low	right, mod
S1	1.00	0.96	0.99	1.00	0.99	0.99	0.99	0.99
S2	0.99	0.97	1.00	1.00	0.96	0.98	1.00	1.00
S3	0.97	0.89	**0.76**	0.97	0.93	0.95	0.92	0.99
S4	0.98	0.92	0.83	0.95	0.97	0.95	0.93	0.99

Table 4.3: Detailed correlation analysis of activation coefficients. The ϱ value means the results of Spearman rank correlation, the p is significance level (calculated by the Fisher-z transformation), and the is the Cohen's d effect size

Synergy		**Resistance**				**Cycling mode**			
		left, only arm	left, arm &leg	right, only arm	right, arm &leg	left, low	left, mod	right, low	right, mod
S1	ϱ	0.84	0.82	0.51	0.78	0.76	0.90	0.59	0.81
	p	0.00	0.00	0.02	0.00	0.00	0.00	0.03	0.00
	d	2.29	2.10	0.91	1.38	2.14	2.29	0.83	2.66
S2	ϱ	0.89	0.74	0.63	0.79	0.80	0.79	0.58	0.71
	p	0.00	0.03	0.01	0.00	0.02	0.01	0.00	0.00
	d	1.42	0.81	1.15	1.43	0.90	0.96	1.50	1.20
S3	ϱ	0.75	0.70	0.93	0.92	0.68	0.74	0.83	0.90
	p	0.00	0.01	0.00	0.00	0.01	0.00	0.00	0.00
	d	1.24	1.00	2.58	2.66	1.08	1.31	2.02	2.86
S4	ϱ	0.79	**0.46**	0.97	0.95	0.65	0.71	0.91	0.94
	p	0.00	0.09	0.00	0.00	0.00	0.02	0.00	0.00
	d	1.35	0.60	4.71	5.01	1.36	0.90	3.71	3.16

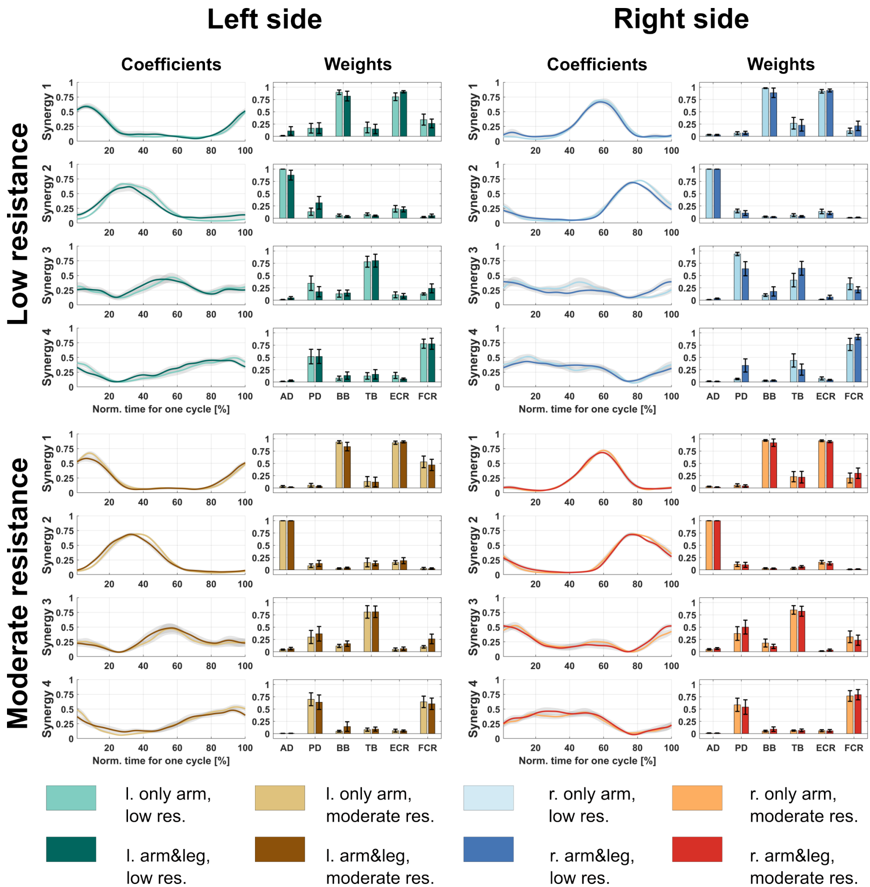

Figure 4.3: Averaged activation coefficients and synergy vectors obtained in eight setups. The activation coefficients are presented as a function of normalized time. The shaded area represent the standard errors. The bar diagrams show the average and standard errors (across participants, n = 10) of muscle weights in each synergy vector.

4.3 Outcomes of hybrid FES cycling training - walking assessment

The biomechanical results of five participants are displayed the following parameters were calculated: *average step length, step time, step speed, average length and jerk of CoP progression and average max. abs GRF components.*

4.3.1 Step length, time, speed

Step length

The average step length of the participants, except p06, are increased after the training and these changes were significant ($p = 0.05$) in case of p01 and p02 participants between the first and the other two assessments. Figure 4.4.

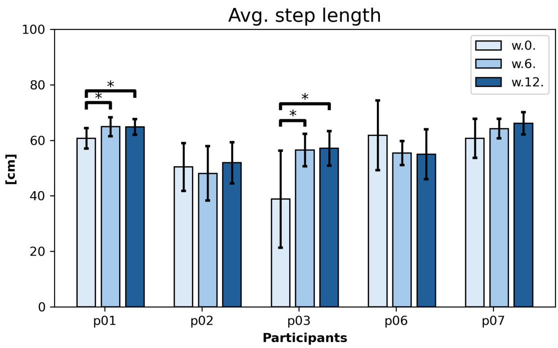

Figure 4.4: Average (across steps) step length and standard deviation of the data prior, at the middle and after the training for the left and the right legs together. The black lines and asterisks denote statistically significant changes between assessments ($p < 0.05$).

Step time

The average step time for all the participants decreased or stayed stable. The changes between the start and the middle state was person specific. Significant changes were before-after the training in case of p01, p03 and p06 and significant changes were between the before-middle states for p01, p02, p03 and p06 patients. See Figure 4.5.

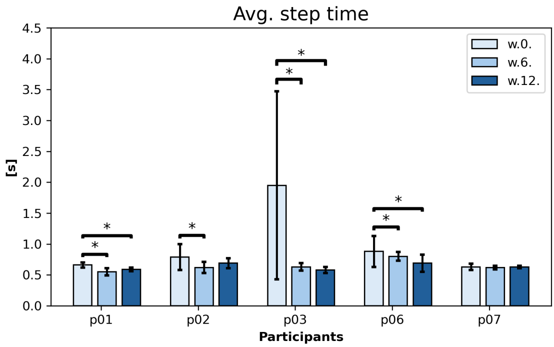

Figure 4.5: Average (across steps) step time and standard deviation of the data prior, at the middle and after the training for the left and the right legs together. The black lines and asterisks denote statistically significant changes between assessments ($p < 0.05$). The three assessments were taken at week 0. (w.0.), week 6. (w.6.) and week 12. (w. 12.).

Step speed

The average step speed for all participants improved and four out of five had significant improvements at least before-after the training. (Figure 4.6). p01, p03, and p06 participants had improvement between the prior and middle states. p03 showed improvement between the middle and after states too.

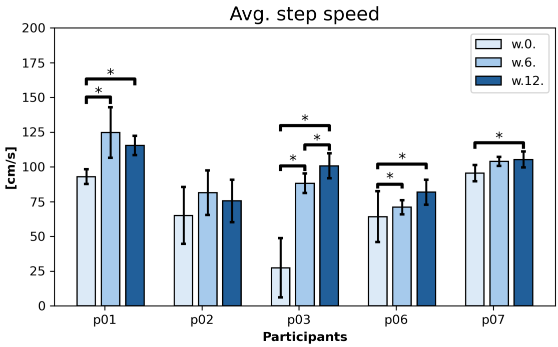

Figure 4.6: Average (across steps) step speed and standard deviation of the data prior, at the middle and after the training for the left and the right legs together. The black lines and asterisks denote statistically significant changes between assessments ($p < 0.05$). The three assessments were taken at week 0. (w.0.), week 6. (w.6.) and week 12. (w. 12.).

4.3.2 CoP progression length and jerk

A statistically significant decreasing in the length of center of pressure (CoP) progression was observed in participants p01, p02, p03, and p07. Participant p06 also exhibited a decrease, but this change did not reach statistical significance. For participant p03, a significant difference was detected between week 0 and week 6. Figure 4.7. The standard deviations of the CoP lengths decreased or remained the same between the before and after the training, except p06 participant.

The average (across steps) total CoP jerk is decreased for all participants. Four out of five had significantly decreasing total jerk from the first to the last assessments and two participant (p01, p03) had significantly decreasing values between the 0th and 6th week measurements. See Figure 4.8.

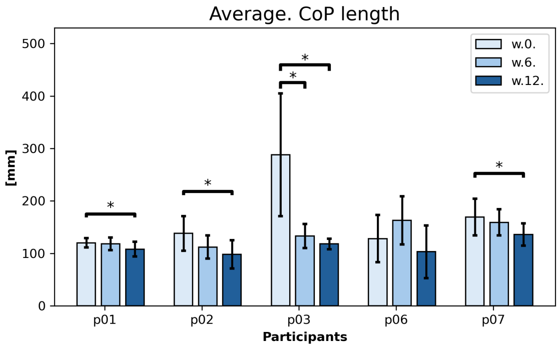

Figure 4.7: Mean (±SD) CoP progression length at weeks 0, 6, and 12. Black lines and asterisks indicate significant differences between time points ($p < 0.05$).

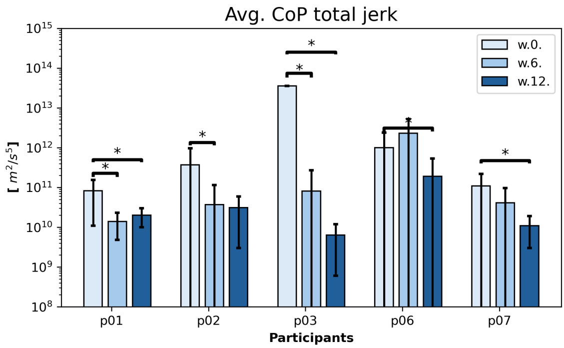

Figure 4.8: Mean (±SD) CoP total jerk at weeks 0, 6, and 12. Black lines and asterisks indicate statistically significant differences between time points ($p < 0.05$).

4.3.3 Ground Reaction Forces

The average maximum of absolute values of ground reaction forces (max. abs. GRF) express the upper boundaries of possible force exertion.

For the **x** (medial-lateral) component of the max. abs. GRF, the changes were personal specific. Significant differences between the measurements were only found in case of p03, at before - middle and before – after states. Difference between the trend of the two sides were observed at p02 and p06. See Figure 4.9.

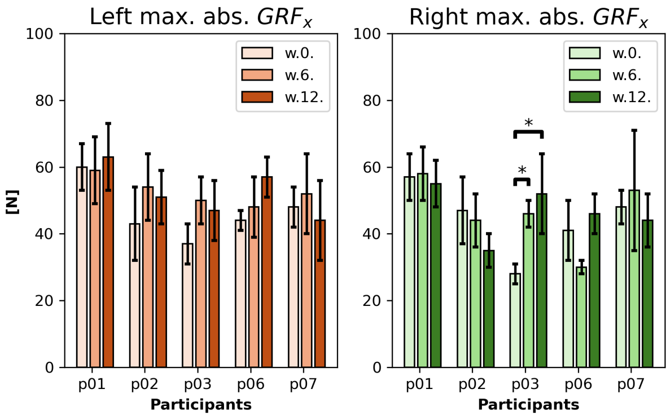

Figure 4.9: Mean (±SD) maximum absolute GRF (x-component) for the left and right legs at weeks 0, 6, and 12. Black lines and asterisks indicate significant differences ($p < 0.05$).

The **y** (anterior posterior) component of the max. abs. GRF were stable or increasing between the week 0. and week 6. Significant changes were found in the before – middle values of p02 for the left side and between the before – after values of p03. See Figure 4.10.

The **z** (vertical) component of the maximum absolute GRF increased significantly for participants p02, p03, and p06 between the first and last assessments. For p01, a significant increase was observed in the left vertical component, while the right remained stable. Only in the case of p07 were there no significant changes in the z component. See Figure 4.11.

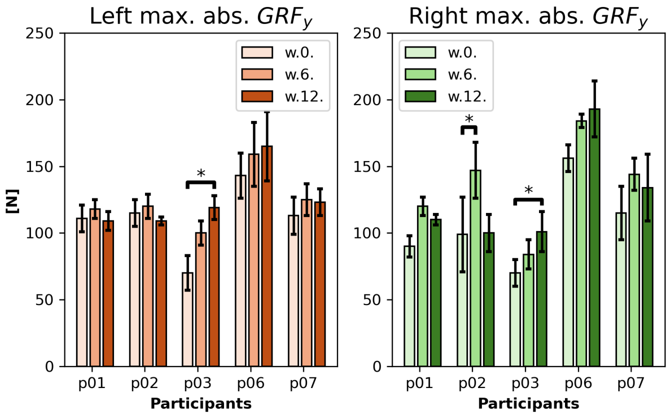

Figure 4.10: Mean (±SD) maximum absolute GRF (y-component) for the left and right legs at weeks 0, 6, and 12. Black lines and asterisks indicate significant differences ($p < 0.05$).

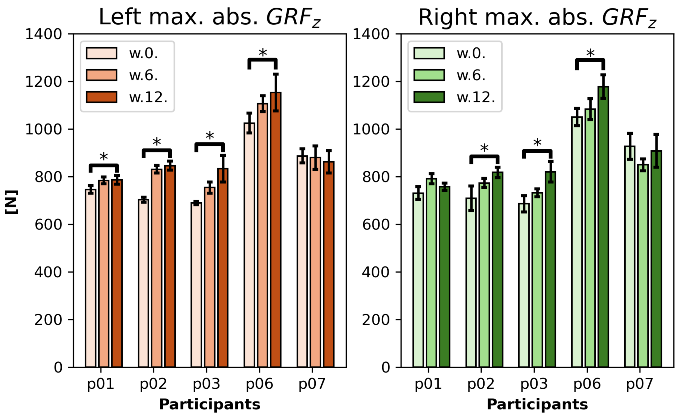

Figure 4.11: Mean (±SD) maximum absolute GRF (z-component) for the left and right legs at weeks 0, 6, and 12. Black lines and asterisks indicate significant differences ($p < 0.05$).

4.3.4 Sample Entropy results

The Sample Entropy (SampEn) is a metric of complexity of a dynamical system. It can describe the periodicity of a timeseries. In our case these time series are the average and standard deviation of step cycle EMG envelopes of the knee flexor and extensor muscles. The results of the five participants are shown in Figure 4.12.

Although there are individual changes of the SampEn, there is a similar trend across the participants. Some preliminary results of this work had been published [C1] at the *IEEE International Conference of Engineering in Medicine and Biology Society (EMBC)*.

p01: SampEn and standard deviation (SD) generally decreased, except for left RF (SampEn) and right Smt (SD). Changes were more pronounced on the right side. p02: Mean values decreased or remained stable, except for right BF. After 12 weeks, SD increased for VL and BF. Bilateral changes were similar in magnitude. p03: Demonstrated the most significant decrease in both SampEn mean and SD across all participants for both sides. p06 (Left): Marked asymmetry between extensors and flexors; flexors showed less regulated activity. RF entropy decreased strongly, VL remained stable, and VM increased slightly (though remained low). Smt and BF values remained high compared to other participants despite a decrease in Smt. SD showed no clear pattern. p06 (Right): More favorable outcomes; all mean and SD values decreased, except for a slight increase in VL. p07: SampEn increased in bilateral RF, left VM, and right Smt. On the left, SD increased (except VL), while on the right, SD decreased (except RF).

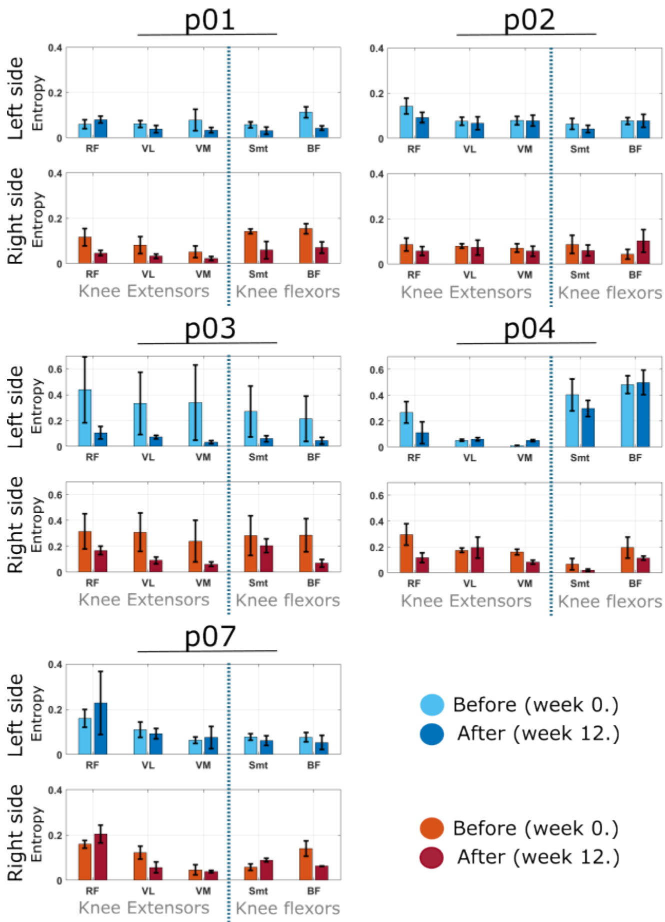

Figure 4.12: Comparison of mean and standard deviation values for Sample Entropy (SampEn) in participant EMG envelopes: Pre- vs. post-hybrid FES cycling training intervention.

5 Discussion

5.1 Arm & leg cycling - neural network

5.1.1 Comparison of the predicted and test EMG signals.

The neural network was partially able to estimate the high-amplitude, spike-like elements of the target EMG signals. These spiking and stochastic phenomena are typical hardly determinable features of EMG activity, which should also be taken into account in the evaluation [26]. In consequence, the introduced prediction examples are smoother than their target signals in Figure 4.1.

Distinction between noise and relevant high frequency features is often difficult. Therefore the networks prefer models with smoother patterns.

Additionally, the use of mean square error (MSE) as a loss function, during the optimization of the network, This metric encourages the network to try to get the expected values of the stochastic process.

The neural network behaves like a low pass filter, which eliminates stochastic and noise-like effects . This may mean that the neural network tries to highlight the general features and patterns of the target signals, which can be beneficial to the construction of a deterministic engineering solution for control.

5.1.2 Comparison of FES activation patterns

The prediction accuracy shows the average performance with standard deviation and is summarized in Table 4.1. Based on the results, the average predictive performance of the system is weak, although there are some better individual results.

5.1.3 Limitations

We suppose that the reasons for the low performance are as follows. Across participants, the EMG variability of the measured muscles is high, which is a commonly appearing problem with this data type. This may suggest different strategies for the implementation of particular cycling tasks. For example, the cycling movement may be maintained by the rhythmic impulse of the quadriceps; therefore, the hamstrings activity could be minimal or where the leg pulls the crank by the hamstrings and pushes it by the quadriceps. To overcome this issue, the involvement of further participants and the increase of model complexity by additional layers or architectural elements would be required.

Another reason for the performance limitation is that the participants were not able to cycle with exactly the same frequency using their upper and lower limbs. Consequently, continuous phase shifting occurred and accumulated across multiple periods. This shifting corrupted the mapping between the upper and lower limb EMG activity. To avoid this effect, further signal processing techniques should be tested to align the upper and lower cycles.

5.2 Arm & leg cycling – muscle synergy analysis

5.2.1 Effect of leg cycling on arm muscle coordination

The main aim of this study was to investigate whether leg cycling, added simultaneously to arm cycling, affects arm muscle synergies in able-bodied people. Our results show that there were no significant differences in the muscle synergy vectors or in the activation coefficients between the 2 cycling modes (only-arm cycling and arm & leg cycling). This suggests that the arm muscle coordination is invariant to leg cycling, and the central nervous system employs the same arm muscle coordination strategy, when lower limb activity is added to the arm cycling movement.

This investigation of arm muscle coordination helps to discern how upper-limb motor control is influenced by lower-limb activity and provides insights into sensorimotor integration and has implications in neurorehabilitation.

The literature on the effects of lower limb cycling on upper limb movements and muscle activation is relatively limited compared with that on the effects of arm cycling on leg muscle activation. One study [27] investigated synergies both for arm cycling and leg cycling but not for simultaneous cycling. Biomechanical and electrophysiological methods have been used to investigate the effects of lower limb cycling on upper limb kinematics and muscle activation, leading to various results [11], [28], [29].

These studies, which investigated the effect of lower limb cycling on arm muscle activation, considered either kinematic or electrophysiological properties of the studied systems and motor tasks. A novelty of our study is that we applied the muscle synergy approach to investigate whether lower limb cycling influences upper limb muscle coordination. Our results support the assumption that lower limb movement does not significantly influence upper limb muscle coordination during arm cycling.

5.2.2 Effect of crank resistance on muscle coordination

We investigated whether different arm crank resistances require different muscle coordination. The results revealed that synergies were not affected by crank resistance in either cycling mode or in either the dominant or non-dominant arm. A previous study showed that variance profiles of muscle activation in arm cranking was not affected by crank resistance [30]. The amplitude of muscle activation (assessed by EMG) increases with higher loads, but the activation profile does not necessarily alter. The EMG signal consists of a combination of activation coefficients and synergy weights, so the magnitude of the activation coefficient is not directly depend on the EMG amplitude. Thus, it is possible that there is a slight difference between the two resistances in both the weights and the activation coefficients, but it is not significant.

[31] found high degrees of similarity among muscle synergies in leg cycling across various load conditions, and demonstrated that different mechanical conditions use the same motor control strategies for cycling. If muscle synergies are shared across load conditions in lower-limb cycling, it is reasonable to assume that similar properties may apply to upper-limb cycling.

5.2.3 Implications for rehabilitation

The common neural control of lower limb and upper limb movements has implications for the rehabilitation of patients with SCI. Dietz [32] posited consequences for rehabilitation of task-dependent neuronal linkage of cervical and thoracic–lumbar propriospinal circuits controlling leg and arm movements. Simultaneous arm and leg cycling is an excellent candidate for rehabilitation therapy for patients with incomplete spinal cord injury [32]. The combination of arm and leg cycling in rehabilitation training protocols may result in higher oxygen uptake than cycling by only two limbs. This is a desired goal of cycling exercises [33], [34]. From the aspect of motor control, our present study suggests that arm muscle coordination is preserved while the CNS controls the cyclist's leg movements in addition to arm movement. Arm cycling control can be maintained when training setups are changing. A previous study revealed that arm configuration variance during arm cranking was not affected by changes in crank resistance

[30]. Our study suggests that arm muscle coordination in terms of muscle synergies is not affected by crank resistance either. Furthermore, muscle coordination in arm cycling does not depend on additional training setups, such as simultaneous leg cycling.

Further studies are needed to investigate arm cycling control during hybrid cycling in people with neurological disorders.

5.3 Hybrid FES cycling training - walking assessment

The length and jerk of the CoP progression curves, it can be observed that the CoP parameters demonstrate a positive development for all patients, with a significant change noted in nearly every instance. These findings suggest that all subjects have improved walking ability, in both step velocity and dynamics.

The change in the maximum absolute values of the Ground Reaction Forces (GRFs) in the x (lateral-medial) and y (anterior-posterior) directions was not statistically significant for any patient, with the exception of subject p03.

However, given the simultaneous increase in step speed, the participants were able to achieve a higher step speed using the same average magnitude of muscular force in the x and y directions. Therefore, the movement became more efficient in these directions.

The vertical (z-direction) Ground Reaction Forces exhibited a significant increase in four out of five cases. It is hypothesized that this increase is attributable to enhanced body support capability.

The changes in SampEn values are in line with the biomechanical parameter changes of participants p01, p02, p03, and p06. Participant p02 showed low SampEn values with mild improvements; this participant had mild, statistically non-significant improvements in other biomechanical parameters as well. In the case of p07, the biomechanical parameters showed improvement, which was not confirmed by the SampEn results.

Excluding the MAS scores and comparing our findings with other clinical assessments, it becomes evident that most clinical tests had lower resolution for describing walking ability than biomechanical measurements.

The SampEn is even measurable even in cases, when MAS score indicates healthy thone (score 0). For example, p03 who had strong SampEn changes. In other cases, such as participants p06 and p07, both metrics changed over the 12-week period, yet their outcomes did not follow the same trend. The interpretation of these features may require further investigation. A few relatively recent but methodologically different work have already begun to address these topics [35], [36].

In summary, the collective analysis of the dynamic and kinematic parameters indicates an improvement in the patients' condition, with individual parameters either remaining stable or showing positive change. These data are in line with the results of clinical test but provide a more detailed resolution of the patients rehabilitation progress.

5.3.1 Comparison with other studies of FES cycling trainings

The study by Yasar et al. [8] involved non-acute individuals with iSCI ($n = 15$). The participants underwent FES cycling training three times a week for one hour per session. The parameters measured in their work included average gait speed (v), step length (l), and stepping cadence (steps/minute), are comparable to the results discussed in the present work. Based on a comparison with the data we collected, the conventional FES leg cycling training demonstrated a slight improvement, showing a 10–15% gain ($\alpha < 0.05$).

In the five individuals we followed up, two out of the five subjects showed a significant improvement in both average step length and average gait speed. However, a significant increase in gait speed was observed in four out of five cases.

It is important to note, that the patients I studied were in the subacute phase of injury, which means they were within the one year post-injury time interval, which constitutes a significant physiological difference.

Our participants had received only the hybrid FES cycling training twice weekly for half an hour per session.

The work most closely related to the one presented here is the article by Zhou et al., which provides detailed changes in clinical, biomechanical, and EMG parameters during the comparison of conventional and hybrid FES cycling training. This study involved seven non-acute individuals with iSCI (incomplete spinal cord injury) who received hybrid FES cycling therapy.

Comparing these results with the findings presented in this thesis, it can be stated that the patients investigated by Zhou et al. started and finished the program with poorer walking ability compared with our participants. It is noteworthy that the patients' average gait velocity increased by 50% based on the 10-meter walk tests, and by 62% based on the biomechanical measurements. The patients investigated by our group, demonstrated a significant 35% step speed improvement. While this rate of improvement is lower than that reported by Zhou et al., several significant differences are observable between the two cohorts. Our protocol used hybrid FES cycling for 30 minutes, twice a week, while Zhou et al. employed a much more intensive protocol of one hour, five times a week. Our patients also started the training in a better baseline condition, which likely accounts for the smaller rate of improvement observed.

The article by Zhou et al. did not report any information on the participants' dynamic gait parameters (GRF and CoP). To the best of our knowledge, the inclusion of these data in the present thesis provides entirely novel findings.

5.3.2 Limitations

A limitation of this section is the current lack of a control group to validate our results. Our research group is actively working on the recruitment and data processing for such a group. However, as a reference, Zhou et al. [3] also investigated the effects of hybrid FES cycling and reported data from a reference group. Based on this information, the positive improvements found in our participants are comparable to the outcomes of their participants who received hybrid FES cycling.

Furthermore, comparative data obtained from able-bodied individuals would provide an interesting basis for comparison as well.

I am also aware that the number of step cycles are small obtained from the gait assessments. A limiting factor in collecting a higher number of step cycles is the physical condition and fatigue of the patients.

6 Conclusion

6.1 New scientific results

Thesis 1.

Question 1, Is there a detectable neural interlimb coordination between the arms and legs during simultaneous arm cranking and leg cycling motor tasks?

Response to Question 1,

The neural network-based approach indirectly indicates that arm muscle activities contain information relevant to the regulation of leg muscles and could be transferred to control leg muscle activities. Conversely, the muscle synergy-based approach detected no significant effect propagating from the legs toward the arms during constant frequency arm and leg cycling. [J2], [J3].

These results are in line with the following interpretation of the common motor control of the upper and lower limbs:

- Beyond reflex-level connections, modulatory influences act primarily from the arms toward the legs during stationary rhythmic arm and leg movements.

Thesis point based on Objective 1a,

I have developed a neural network which was capable of learning and estimating the activity of specific knee extensor and flexor muscles based on the EMG activity of the arm muscles. Although the prediction accuracy was insufficient to generate a unipolar FES (Functional Electrical Stimulation)

stimulation pattern, further refinement remains highly relevant for the automation of muscle stimulation during FES assisted leg cycling.

The accuracy of the model's learning capabilities was primarily limited by the inconsistent frequency and phase synchronization between the arms and legs, caused by natural movement variability and fluctuations in the subjects' attention. Despite these factors, the neural network demonstrated partial learning, suggesting that EMG data collected from the arms can be utilized—at least partially—to control leg muscles during simultaneous arm and leg cycling tasks. Given that this study utilized a relatively small and limited dataset across multiple subjects, it can be assumed that the significantly more complex architecture of the nervous system may also be capable of co-controlling the arm and leg muscles [J2].

Thesis point based on Objective 1b,

I have found no statistically significant differences in upper-limb muscle synergies between arm cranking alone and simultaneous arm and leg cycling at a steady-state cadence, using Non-Negative Matrix Factorization (NNMF) for the analysis. However, these findings do not exclude the reflex-level modulation or modulation of upper-limb motor control induced by the variable-frequency movement of the lower extremities [J3].

Thesis 2.

Question 2, How do the ground reaction forces during walking change in case of incomplete spinal cord injured participants who, in addition to the conventional rehabilitation therapies, participated in simultaneous voluntary arm cranking and functional electrical stimulation-assisted leg cycling (hybrid FES cycling) training?

Thesis point based on Question 2,

I have designed a measurement protocol to discern gait characteristics and I have presented the changes of ground reaction force related dynamic parameters in particular the length and smoothness of center of pressure (CoP) progression in cases of iSCI participants who received hybrid FES cycling training. After twelve weeks, the GRF was acting more consistently on a shorter and smoother paths for all participants compared to the initial values. These results also support that the walking ability of the participants become more stable and controlled [C1], [C2], [C3], [C4].

I have pointed out that the lengths of CoP progression curves decreased for all participants and the changes were significant for four out of five participants at the end of the training based on the combined data from both sides. Similarly, CoP total jerk decreased for all patients, with the reduction being significant in four out of five cases according to the combined data from both sides.

My analysis indicates that the medio-lateral (x-axis) components of the GRF show individual-specific variations in the changes of maximum absolute values. For the anterio-posterior (y-axis) components, results showed either stagnation or a slight increase between the beginning and the end of the training. Regarding the vertical (z-axis) components, three out of five subjects showed a clear significant increase, while one subject exhibited a significant increase specifically in the left leg. One subject showed stagnation or a slight decrease in this parameter.

Based on these results, the increase in force production is primarily characteristic of the vertical component. This suggests an enhanced capacity for weight-bearing during gait. Meanwhile, the time course of the application point of the GRF became smoother. When interpreted alongside classical biomechanical parameters and clinical scores, my findings indicate that patients' walking ability became more stable while their gait speed increased.

6.2 The relevance of the results

By predicting lower limb muscle activity from upper limb EMG signals, a novel FES-control method was developed. These preliminary results establish a foundation for real-world clinical applications.

Investigating muscle synergies revealed that simultaneous leg cycling does not influence arm synergies. This suggests a unidirectional information flow from arms to legs (proximal to distal) or interaction only during phase/frequency shifts, providing a basis for tetraplegic physiotherapy design.

Evaluation of hybrid FES cycling as a low-intensity supplementary training for iSCI patients showed positive effects on walking ability. While absolute improvements were smaller than in previous studies (e.g., Zhou et al.), the relative improvement per time-intensity was higher, confirming the training's efficiency despite its unclear underlying mechanisms.

6.3 Future plan

I will investigate the bidirectional mapping between upper and lower limb EMG signals. To ensure consistency, segmented EMG periods from cycling will be phase-aligned during preprocessing. Additionally, the dataset will be expanded with data from more participants to enhance the neural network's generalization and learning performance.

While Non-negative Matrix Factorization (NMF) is standard for modeling muscle co-activation, it often fails to capture transitions and gradual temporal trends. To overcome this, I will apply Tensor Factorization. Unlike NMF, this method utilizes a third matrix to describe the temporal variations of muscle synergies. This approach will provide critical insights into the reciprocal influence of upper and lower limbs, particularly during changes in cycling frequency or phase.

I will further evaluate the effects of Hybrid FES-cycling on the walking ability of individuals with incomplete spinal cord injury (iSCI) by increasing the sample size and establishing a control group. Furthermore, I will compare these results with stroke patient data from the OpenGait database. This comparative analysis aims to identify injury-specific EMG and biomechanical features across different hierarchical levels of neurological impairment.

List of Publications

List of journal publications

[J1] M. Mravcsik, A. Fodor, **B. Radeleczki**, M. Feher, P. Cserhati, A. Klauber, J. Laczko, and L. Botzheim, "Retrospective analysis of cardiovascular effects of fes cycling in people with complete and incomplete spinal cord injury", *Journal of Clinical Medicine*, vol. 15, no. 5, p. 1967, 2026.

[J2] **B. Radeleczki**, M. Mravcsik, L. Bozheim, and J. Laczko, "Prediction of leg muscle activities from arm muscle activities in arm and leg cycling", *The Anatomical Record*, vol. 306, no. 4, pp. 710–719, 2023.

[J3] L. Botzheim, **B. Radeleczki**, M. Mravcsik, J. L. Pons, F. O. Barroso, and J. Laczko, "Assessment of the influence of lower limb cycling on arm muscle coordination during upper limb cycling – a pilot study", *Journal of NeuroEngineering and Rehabilitation*, 2026, In press.

List of conference publications

[C1] L. Botzheim, **B. Radeleczki**, M. Feher, P. Cserhati, and J. Laczko, "Computational methods to support clinical assessment in examination of walking ability", in *2025 47th Annual International Conference of the IEEE Engineering in Medicine and Biology Society (EMBC)*, IEEE, 2025, pp. 1–6.

[C2] **B. Radeleczki**, M. Feher, M. Mravcsik, J. Laczko, J. L. Pons, and L. Botzheim, “Kinesiological gait parameter changes in two incomplete spinal cord injured patients due to hybrid arm and leg cycling therapy–pilot study”, in *International Conference on NeuroRehabilitation*, Springer, 2024, pp. 15–19.

[C3] **B. Radeleczki**, L. Botzheim, N. Nagy, J. Laczko, and M. Mravcsik, “Change of ground reaction force and center of pressure in walking of spinal cord injured patients after fes cycling training”, in *Progress in Clinical Motor Control II.*, Shirley Ryan AbilityLab, 2023, p. 120.

[C4] L. Botzheim, **B. Radeleczki**, A. Fodor, M. Feher, and J. Laczko, “Jerk analysis of gait in persons with incomplete spinal cord injury: A study about the effect of hybrid arm and leg cycling”, in *International Scientific Conference Motor Control 2024: From Theory To Applications*, The International Society of Motor Control, 2024, p. 16.

References

[1] N. S. C. I. Center, “Spinal cord injury facts and figures at a glance”, *The journal of spinal cord medicine*, vol. 37, no. 3, pp. 355–356, 2014.

[2] V. K. Noonan, “A look at spinal cord injury in canada: Rick hansen spinal cord injury registry (rhscir)–2021 sci data summary”, *Topics in Spinal Cord Injury Rehabilitation*, vol. 29, no. Supplement, pp. 165–170, 2023.

[3] R. Zhou, L. Alvarado, R. Ogilvie, S. L. Chong, O. Shaw, and V. K. Mushahwar, “Non-gait-specific intervention for the rehabilitation of walking after sci: Role of the arms”, *Journal of Neurophysiology*, vol. 119, no. 6, pp. 2194–2211, 2018.

[4] D. Barbosa, C. P. Santos, and M. Martins, “The application of cycling and cycling combined with feedback in the rehabilitation of stroke patients: A review”, *Journal of Stroke and Cerebrovascular Diseases*, vol. 24, no. 2, pp. 253–273, 2015.

[5] F. O. Barroso, D. Torricelli, J. C. Moreno, J. Taylor, J. Gomez-Soriano, E. Bravo-Esteban, S. Piazza, C. Santos, and J. L. Pons, “Shared muscle synergies in human walking and cycling”, *Journal of neurophysiology*, vol. 112, no. 8, pp. 1984–1998, 2014.

[6] T. Klarner, T. S. Barss, Y. Sun, C. Kaupp, and E. P. Zehr, “Preservation of common rhythmic locomotor control despite weakened supraspinal regulation after stroke”, *Frontiers in integrative neuroscience*, vol. 8, p. 95, 2014.

[7] P. Ditunno and J. Dittuno, “Walking index for spinal cord injury (wisci ii): Scale revision”, *Spinal cord*, vol. 39, no. 12, pp. 654–656, 2001.

[8] E. Yaşar, B. Yılmaz, S. Göktepe, and S. Kesikburun, “The effect of functional electrical stimulation cycling on late functional improvement in patients with chronic incomplete spinal cord injury”, *Spinal Cord*, vol. 53, no. 12, pp. 866–869, 2015.

[9] L. D. Duffell and N. d. N. Donaldson, “A comparison of fes and scs for neuroplastic recovery after sci: Historical perspectives and future directions”, *Frontiers in neurology*, vol. 11, p. 607, 2020.

[10] E. P. Zehr, M. Klimstra, E. A. Johnson, and T. J. Carroll, “Rhythmic leg cycling modulates forearm muscle h-reflex amplitude and corticospinal tract excitability”, *Neuroscience letters*, vol. 419, no. 1, pp. 10–14, 2007.

[11] M. Sakamoto, T. Tazoe, T. Nakajima, T. Endoh, S. Shiozawa, and T. Komiyama, “Voluntary changes in leg cadence modulate arm cadence during simultaneous arm and leg cycling”, *Experimental brain research*, vol. 176, no. 1, pp. 188–192, 2007.

[12] M. Sakamoto, T. Endoh, T. Nakajima, T. Tazoe, S. Shiozawa, and T. Komiyama, “Modulations of interlimb and intralimb cutaneous reflexes during simultaneous arm and leg cycling in humans”, *Clinical neurophysiology*, vol. 117, no. 6, pp. 1301–1311, 2006.

[13] R. Zhou, L. Alvarado, S. Kim, S. L. Chong, and V. K. Mushahwar, “Modulation of corticospinal input to the legs by arm and leg cycling in people with incomplete spinal cord injury”, *Journal of neurophysiology*, vol. 118, no. 4, pp. 2507–2519, 2017.

[14] T. Lin, B. G. Horne, P. Tino, and C. L. Giles, “Learning long-term dependencies in narx recurrent neural networks”, *IEEE transactions on neural networks*, vol. 7, no. 6, pp. 1329–1338, 1996.

[15] F. Hug, "Can muscle coordination be precisely studied by surface electromyography?", *Journal of electromyography and kinesiology*, vol. 21, no. 1, pp. 1–12, 2011.

[16] L. Botzheim, J. Laczko, D. Torricelli, M. Mravcsik, J. L. Pons, and F. Oliveira Barroso, "Effects of gravity and kinematic constraints on muscle synergies in arm cycling", *Journal of neurophysiology*, vol. 125, no. 4, pp. 1367–1381, 2021.

[17] N. A. Turpin, S. Uriac, and G. Dalleau, "How to improve the muscle synergy analysis methodology?", *European journal of applied physiology*, vol. 121, no. 4, pp. 1009–1025, 2021.

[18] D. D. Lee and H. S. Seung, "Learning the parts of objects by non-negative matrix factorization", *nature*, vol. 401, no. 6755, pp. 788–791, 1999.

[19] F. Hug, N. A. Turpin, A. Guével, and S. Dorel, "Is interindividual variability of emg patterns in trained cyclists related to different muscle synergies?", *Journal of applied physiology*, vol. 108, no. 6, pp. 1727–1736, 2010.

[20] Y.-X. Wang and Y.-J. Zhang, "Nonnegative matrix factorization: A comprehensive review", *IEEE Transactions on knowledge and data engineering*, vol. 25, no. 6, pp. 1336–1353, 2012.

[21] J. S. Richman, D. E. Lake, and J. R. Moorman, "Sample entropy", in *Methods in enzymology*, vol. 384, Elsevier, 2004, pp. 172–184.

[22] P. Konrad, "The abc of emg", *A practical introduction to kinesiological electromyography*, vol. 1, no. 2005, pp. 30–5, 2005.

[23] J. S. Richman and J. R. Moorman, "Physiological time-series analysis using approximate entropy and sample entropy", *American journal of physiology-heart and circulatory physiology*, vol. 278, no. 6, H2039–H2049, 2000.

[24] K. M. Steele, M. E. Munger, K. M. Peters, B. R. Shuman, and M. H. Schwartz, "Repeatability of electromyography recordings and muscle synergies during gait among children with cerebral palsy", *Gait & posture*, vol. 67, pp. 290–295, 2019.

[25] H. Li and Q. Rong, "Cost function criteria using muscle synergies: Exploring the potential of muscle synergy hypothesis", *Computer Methods and Programs in Biomedicine*, vol. 250, p. 108 170, 2024.

[26] K. Nazarpour, A. H. Al-Timemy, G. Bugmann, and A. Jackson, "A note on the probability distribution function of the surface electromyogram signal", *Brain research bulletin*, vol. 90, pp. 88–91, 2013.

[27] T. Cartier, G. Rao, E. Viehweger, and L. Vigouroux, "Evolution of muscle coordination and mechanical output following four weeks of arm cranking submaximal training.", *Journal of Neurophysiology*, 2023.

[28] M. Sakamoto, T. Tazoe, T. Nakajima, T. Endoh, and T. Komiyama, "Leg automaticity is stronger than arm automaticity during simultaneous arm and leg cycling", *Neuroscience Letters*, vol. 564, pp. 62–66, 2014.

[29] S. K. Sidhu, J. C. Weavil, M. Venturelli, R. S. Garten, M. J. Rossman, R. S. Richardson, B. S. Gmelch, D. E. Morgan, and M. Amann, "Spinal μ-opioid receptor-sensitive lower limb muscle afferents determine corticospinal responsiveness and promote central fatigue in upper limb muscle", *The Journal of physiology*, vol. 592, no. 22, pp. 5011–5024, 2014.

[30] M. Mravcsik, L. Botzheim, N. Zentai, D. Piovesan, and J. Laczko, "The effect of crank resistance on arm configuration and muscle activation variances in arm cycling movements", *Journal of Human Kinetics*, vol. 76, p. 175, 2021.

[31] J. Esmaeili and A. Maleki, “Comparison of muscle synergies extracted from both legs during cycling at different mechanical conditions”, *Australasian physical & engineering sciences in medicine*, vol. 42, no. 3, pp. 827–838, 2019.

[32] V. Dietz, “Do human bipeds use quadrupedal coordination?”, *Trends in neurosciences*, vol. 25, no. 9, pp. 462–467, 2002.

[33] S. Coupaud, H. Gollee, K. Hunt, M. Fraser, D. Allan, and A. McLean, “Arm-cranking exercise assisted by functional electrical stimulation in c6 tetraplegia: A pilot study”, *Technology and Health Care*, vol. 16, no. 6, pp. 415–427, 2008.

[34] C. Zinner, B. Sperlich, D.-P. Born, and G. Michels, “Effects of combined high intensity arm and leg training on performance and cardio-respiratory measures.”, *The Journal of sports medicine and physical fitness*, vol. 57, no. 7-8, pp. 969–975, 2016.

[35] T. Xie, Y. Leng, Y. Zhi, C. Jiang, N. Tian, Z. Luo, H. Yu, and R. Song, “Increased muscle activity accompanying with decreased complexity as spasticity appears: High-density emg-based case studies on stroke patients”, *Frontiers in Bioengineering and Biotechnology*, vol. 8, p. 589 321, 2020.

[36] X. Tang, X. Zhang, X. Gao, X. Chen, and P. Zhou, “A novel interpretation of sample entropy in surface electromyographic examination of complex neuromuscular alternations in subacute and chronic stroke”, *IEEE Transactions on Neural Systems and Rehabilitation Engineering*, vol. 26, no. 9, pp. 1878–1888, 2018.